Broad-Band Microwave Measurements with Transient Radiation from Optoelectronically Pulsed Antennas

G. ARJAVALINGAM, MEMBER, IEEE, YVON PASTOL, JEAN-MARC HALBOUT, MEMBER, IEEE, AND GERARD V. KOPCSAY, MEMBER, IEEE

Abstract —A broad-band microwave measurement technique based on picosecond transient radiation from optoelectronically pulsed antennas is described. It is performed with exponentially tapered coplanar stripline antennas which are integrated with the photoconductive devices used for ultrafast pulse generation and sampling. The signal analysis required for deriving the desired physical properties from the measured time-domain waveforms is discussed. This is a coherent technique that independently determines both the real and the imaginary parts of the dielectric constants of materials, from 10 to 130 GHz, in a single experiment. Some representative results are presented.

I. Introduction

OVER THE past decade the field of picosecond optoelectronics has advanced from an exploratory science to a powerful measurement technique [1]. With the advent of reliable sources of ultrashort optical pulses and high-speed detectors, photoconductive sampling has been effectively used to characterize fast electronic devices [2], circuits [3], and transmission-line structures used to interconnect these circuits [4]. Since electrical pulses with durations of only a few picoseconds have frequency components extending from zero to more than 100 GHz, they can also be useful for microwave measurements over this wide bandwidth. In this paper we discuss such an application of picosecond optoelectronics, namely broad-band microwave measurements with freely propagating transient radiation launched by photoconductivity-generated electrical pulses [5]. Many microwave and millimeter-wave measurement techniques, such as the cavity perturbation method, are only applicable at discrete frequencies [6]. Furthermore, conventional broad-band measurements are dependent upon the availability of tunable sources and suitable detectors. The tuning ranges of traditional microwave devices are at best 20 GHz [6], [7], and for wide frequency coverage (0–100 GHz) several sets of equipment are required. Although techniques such as dispersive Fourier transform spectroscopy are truly broad-band [8], their frequency coverage does not usually extend below 120 GHz. Hence, there is a particular need for broad-band measurement methods in the 0–100 GHz frequency range. For example, the increasing speed of digital electronics has intensified the need to understand the dielectric properties of materials used to carry signals containing frequency components up to 100 GHz.

The coherent microwave transient spectroscopy (COMITS) technique described in this paper is based on electromagnetic pulses radiated and received by broad-band antennas integrated directly with high-speed optoelectronic devices [9]. Ultrashort optical pulses are used to generate the picosecond-duration electrical pulses which drive the antennas and also to photoconductively sample the received waveforms. No traditional microwave sources or detectors are used in the entire experiment. Our current frequency coverage is from ~10 GHz to more than 125 GHz with 5 GHz frequency resolution. This quasi-optical technique is coherent by nature, and consequently measures both the real and the imaginary part of the dielectric constant of a material in a single experiment. The paper is organized as follows: We first describe the experimental apparatus and discuss the signal analysis that permits coherent broad-band microwave measurements. We then discuss the factors which limit the accuracies of the dielectric measurements carried out using this technique. Some improvements to the basic setup are described, followed by results obtained with the modified apparatus. These results include the complex transmission function of Fabry–Pérot interferometers which have well known and predictable behavior, and the dielectric properties (loss and dispersion) of Plexiglas,[1] a typical low-loss material. The paper is then summarized.

II. Experiments

The basic COMITS experimental setup is shown schematically in Fig. 1. It consists of a transmitting antenna and an identical receiving antenna with the sample to be characterized located between them. A coplanar-strip feedline is terminated at one end by bonding pads, for external connections, and is exponentially flared at the other end to form the radiating element. The strip width, spacing, and length of the feedline are respectively 5 μm,

Manuscript received April 21, 1989; revised November 12, 1989.
The authors are with the T. J. Watson Research Center, IBM Research Division, P.O. Box 218, Yorktown Heights, NY 10598.
IEEE Log Number 8934041.

[1] Plexiglas is a trademark of the Rohm and Haas Company, Philadelphia

0018-9480/90/0500-0615$01.00

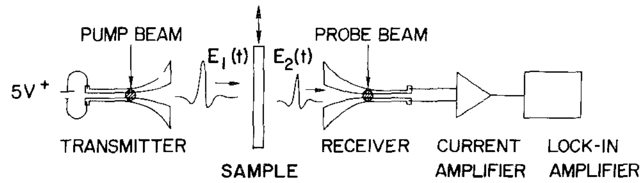

Fig 1 Schematic of the COMITS experimental setup The electric fields shown are defined in the text

10 μm, and 4 mm. The antenna itself is 3.7 mm long and has an end opening of 2.6 mm as measured from the outside edges of the metallization [10]. The entire structure is photolithographically fabricated directly on a silicon on sapphire substrate [11]. The silicon epilayer is then implanted with O^+ ions at energies of 100 and 200 keV with dosages of $1 \cdot 10^{15}/cm^2$ at each energy. The ion implantation creates defects in the silicon resulting in a reduction of the carrier lifetime to less than 1 ps [12]. The semiconductor layer is illuminated by a focused beam of picosecond optical pulses of a suitable wavelength. The electron–hole pairs generated at the point of illumination result in current pulses which also have picosecond durations [13].

We use exponentially tapered coplanar stripline antennas in our experiments because of their broad bandwidth, directivity, and transmission-line natures [14]. The broad bandwidth is a consequence of the fact that each section of the exponential taper radiates efficiently at a frequency where the lateral dimension corresponds to half a wavelength. Since the main lobe of the antenna radiation pattern is directed close to the longitudinal direction [10], no appreciable phase shift occurs between the pulse propagating on the antenna structure and the radiated field. Consequently, there is little dispersion and the radiated pulse has a short time duration. Finally, the transmission line nature of these structures ensures that the pulses reflected from the ends are separated by long times from the main pulse. This facilitates signal analysis, since the delay and attenuation of the main pulse can be studied without interference from the reflected pulses.

A continuous train of picosecond optical pulses is divided into two beams of equal intensity; one is used to excite the transmitter (pump), the other to photoconductively sample (probe) the received voltage. A frequency-doubled, pulse-compressed, mode-locked Nd:YAG laser is the source of 2.5-ps-wide optical pulses which have an average power of 250 mW at 100 MHz repetition rate [15]. The experiments are carried out as follows: the transmitter is biased with a dc voltage (5–6 V), and is excited with the pump beam to photoconductively generate short current pulses at the edge of the antenna. Each pulse radiates as it propagates in the antenna section. The field incident on the receiver induces a transient voltage across its feedline which is photoconductively sampled, as a function of time, by the suitably delayed probe beam [13]. The pump beam is mechanically chopped while the receiver is attached to low-speed lock-in detection electronics for signal averaging. No conventional microwave sources or detectors are used. The high-speed, broad-band nature of the experiment is contained within the optical pump and probe pulses.

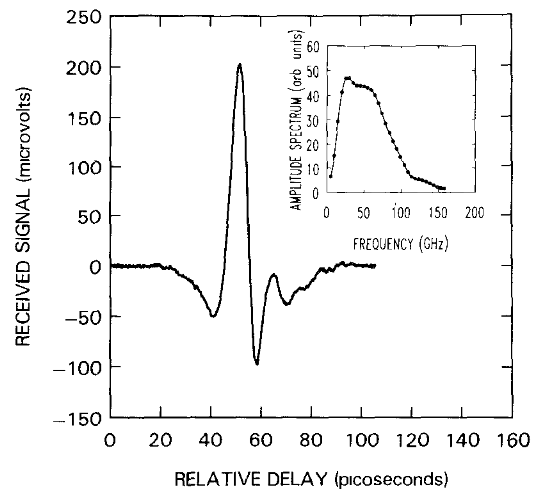

Fig 2. Received waveform with no sample between the transmitter and the receiver The corresponding amplitude spectrum is shown in the inset. The dots in the spectrum are determined from the experimental data; the continuous line is a guide to the eye

A typical received waveform for an antenna separation of 4 cm is shown in Fig. 2 together with its amplitude spectrum obtained by a numerical Fourier transform. The inverse dependence of the received voltage amplitude on the antenna separation verifies that, at this distance, the receiving antenna is in the far field of the transmitting antenna [10]. The spectrum has components extending up to 150 GHz and, as expected, vanishes towards zero frequency. It is broadly peaked around 60 GHz, which is the resonant frequency of the end opening. Since the measured time-dependent waveform is proportional to the received field, phase information is preserved. This is in contrast to many other microwave measurement techniques where power is detected with square-law detectors, and phase information is lost. Details of the transient radiation properties of the antennas used here have been discussed elsewhere [10]. We briefly mention that the bandwidth is increased and the efficiency decreased for an antenna with smaller end opening. We also determined experimentally that the radiation is highly polarized with the electric field parallel to the substrate surface [10].

III. Theory

The COMITS technique is used to characterize the broad-band complex transmission function of a sample in the following manner. A recording is first taken ($v_1(t)$) without any sample between the transmitter and the receiver. Then the sample is inserted close to the receiver and a second recording ($v_2(t)$) is taken. The cross section of the samples should be larger than the beam size to avoid diffraction at the sample edges. It should also be greater than the cross section of the receiving pattern at the sample position so that the voltage induced on the receiver is due only to fields that have propagated through the sample. From measurements of the beam pattern [10] we estimate the required minimum lateral dimensions for transmission experiments to be 3.0 cm, and in all our measurements samples with 5 cm (or larger) clear apertures were used.

For the purpose of this discussion we define the reception and photoconductive sampling (which is analogous to electronic sampling) as a single time-dependent window function $S(t)$. If $E_1(t)$ and $E_2(t)$ are, respectively, the fields incident on the receiver without and with the sample present (see Fig. 1), then

$$v_i(t) = \int_{-\infty}^{\infty} E_i(t') \cdot S(t'-t)\, dt', \qquad i=1,2. \tag{1}$$

That is, the measured voltage waveforms are correlations (and not convolutions) of the incident fields with the sampling function. We define the Fourier transforms of the time-dependent signals (operator $\boldsymbol{F}$) as

$$\boldsymbol{F}\{E_i(t)\} = \tilde{E}_i(f) = E_i(f)\, e^{-j\Phi_{E_i}(f)}, \qquad i=1,2$$

$$\boldsymbol{F}\{S(t)\} = \tilde{S}(f) = S(f)\, e^{-j\Phi_S(f)}$$

and

$$\boldsymbol{F}\{v_i(t)\} = \tilde{V}_i(f) = V_i(f)\, e^{-j\Phi_{V_i}(f)}, \qquad i=1,2.$$

If the frequency-dependent complex transmission function of the sample is

$$\tilde{H}(f) = H(f)\, e^{-j\Phi_H(f)}$$

then

$$\tilde{E}_2(f) = \tilde{H}(f) \cdot \tilde{E}_1(f) \tag{2}$$

since transmission through a sample is a product operation in the frequency domain (denoted by variable f). The only assumption made is that transmission through the sample is linear in field, which is true for the weak fields and the materials used here. From elementary Fourier analysis and (1) and (2), it can be shown that

$$\tilde{V}_1(f) = \tilde{E}_1(f) \cdot \{\overline{\tilde{S}(f)}\} \tag{3}$$

and

$$\tilde{V}_2(f) = \tilde{E}_2(f) \cdot \{\overline{\tilde{S}(f)}\} = \tilde{H}(f) \cdot \tilde{E}_1(f) \cdot \{\overline{\tilde{S}(f)}\} \tag{4}$$

where $\overline{\tilde{S}(f)}$ is the complex conjugate of $\tilde{S}(f)$ [16]. Therefore, it follows from (3) and (4) that

$$\tilde{H}(f) = \frac{\tilde{V}_2(f)}{\tilde{V}_1(f)} \tag{5}$$

or, in terms of amplitudes and phases,

$$H(f) = \frac{V_2(f)}{V_1(f)} \tag{6}$$

and

$$\Phi_H = \Phi_{V2}(f) - \Phi_{V1}(f). \tag{7}$$

The only requirement on the physics of the picosecond photoconductive pulse generation scheme is that the received signal be a linear function of voltage. If it were not linear then the received waveforms $V_{1,2}(t)$ would have a nonlinear relationship to the amplitude of the incident fields $E_{1,2}(t)$ and (1) and (2) would not be valid. We checked the linearity of our setup by plotting the peak of the measured waveforms as a function of the bias voltage applied to the transmitting antenna, in the absence of a sample (Fig. 3). The points fall along a straight line within the 2% margin of error which arises from fluctuations of the laser power. We also measured the average current from the photoconductive switches as a function of the incident optical power and again observed a linear relationship to the maximum pump power (180 mW) used in our experiments.

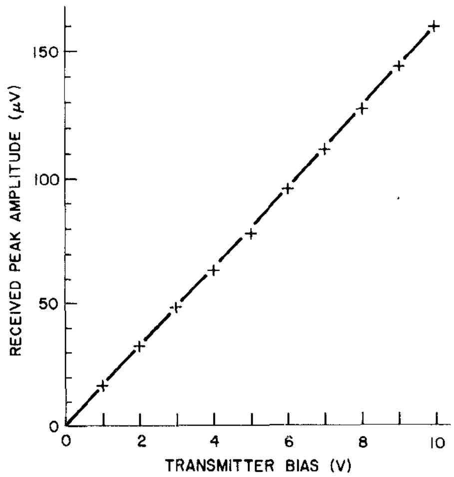

Fig. 3. The peak amplitude of the received signal plotted as a function of the bias voltage applied to the transmitter.

The measured time-dependent waveforms are truncated, to avoid the influence of any unwanted reflections, before Fourier analysis. The spectral resolution of the measurements is determined by the time extent of the experimentally obtained points. In addition, the low-frequency coverage will be improved considerably by extending the reflection-free time window. For the measurements discussed in this paper the separation of the spectral points is 5 GHz, since a fast Fourier transform algorithm with 1024 points is used at a point spacing of 0.2 ps.

In order to obtain frequency-dependent dielectric properties, waveforms are recorded with two different pieces of material. These pieces are chosen to be of sufficient thickness so that pulses from multiple reflections at the sample surfaces fall outside the time span of the main pulse. This avoids the so-called channel fringes [17], which are related to the fact that the samples behave as low-finesse Fabry–Pérot interferometers. In our measurements, samples with thicknesses from 5 mm to 20 mm were used. The material samples should also have appropriately large lateral dimensions, as discussed before. Using the previous definitions, the waveforms A_1 and A_2 recorded with sample thicknesses l_1 and l_2 are written as

$$\boldsymbol{F}\{A_1(t)\} = \tilde{A}_1(f) = A_1(f)\, e^{-j\Phi_1(f)}$$

and

$$\boldsymbol{F}\{A_2(t)\} = \tilde{A}_2(f) = A_2(f)\, e^{-j\Phi_2(f)}$$

where $l_2 > l_1$. Transmission through each sample results in both an absorption and a delay within the bulk of the material and reflections at the end surfaces. Ignoring the multiple reflections which are removed by time windowing as discussed above, the latter effect is the same for both samples. Thus, we obtain the effect of propagation through material of thickness $l_2 - l_1$ by

$$\tilde{H}_{l_2-l_1}(f) = \frac{\tilde{A}_2(f)}{\tilde{A}_1(f)} = \frac{A_2(f)}{A_1(f)} e^{-j\{\Phi_2(f)-\Phi_1(f)\}} \quad (8)$$

where the effect of the reflections at the end surfaces cancels out. If the frequency-dependent electric field absorption coefficient per unit length of the material is given by $\alpha_E(f)$ and the microwave refractive index is given by $n(f)$, it follows from (8) that

$$\alpha_E(f) = \frac{-1}{(l_2 - l_1)} \ln\left\{\frac{A_2(f)}{A_1(f)}\right\} \quad (9)$$

and

$$n(f) = 1 + \frac{c}{2\pi f(l_2 - l_1)}\{\Phi_2(f) - \Phi_1(f)\} \quad (10)$$

where c is the microwave velocity in free space. The dielectric constant $\epsilon(f)$ and the power loss coefficient $\alpha(f)$ are then given by

$$\epsilon(f) = n^2(f) \quad (11)$$

and

$$\alpha(f) = 2\alpha_E(f). \quad (12)$$

It can now be clearly seen that since phase information is preserved in the measurements, the technique is indeed coherent, and we obtain both the dispersion and the loss properties of materials, over a wide frequency range, in a single experiment. This contrasts with some traditional dielectric characterization methods where the loss spectrum is determined from power loss measurements, and the dispersion spectrum is then derived through the Kramers–Kronig relations.

The initial measurements of the dielectric properties of materials using the COMITS technique were carried out with samples of 10–16 mm thickness [5]. When thick samples are used with a noncollimated beam a correction is necessary to account for the refraction occurring at the sample surfaces [18]. This is illustrated in Fig. 4, where it can be observed that the refraction of the diverging beam effectively moves the apparent origin of the radiation closer to the receiver. The correction is then a renormalization of the received field by this reduced antenna separation. An approximate value can be derived from simple considerations of geometrical optics and is given by

$$\Delta r = l \cdot \left\{1 + \frac{\cos\theta}{n\cos\theta_1}\right\} \quad (13)$$

where l is the sample thickness and n its nominal microwave index; θ is the half-angle of the main lobe of the radiation pattern, which was determined to be 15° for the

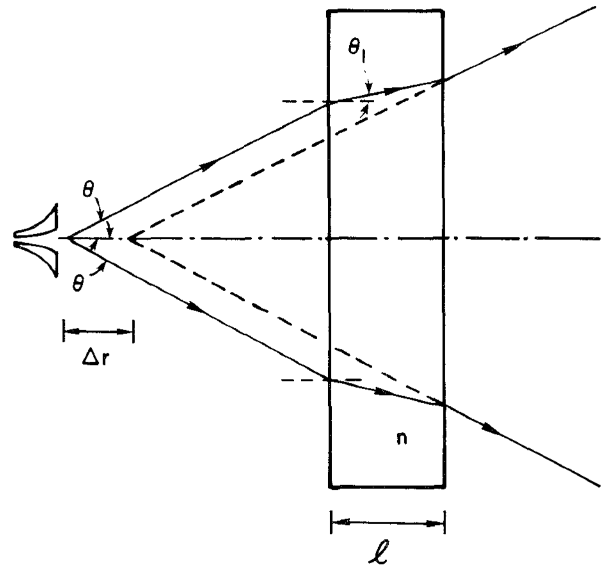

Fig. 4. Schematic representation of the refraction that occurs when diverging beams propagate through thick samples.

antennas used in our experiments [10]. The angle θ_1 is defined in Fig. 4.

Since the source of the phase spectrum is the delay associated with the waveforms, and loss is determined from the reduction in the amplitude, the accuracy of our measurements can be determined from the known characteristics of the experimental apparatus. The resolution in the refractive index measurements (Δn) is derived from (10) to be

$$\frac{\Delta n}{n} = \frac{2c\Delta t}{nl} + 2\frac{\Delta l}{l} \quad (14)$$

where l is the difference in sample thicknesses, Δl is its uncertainty, and Δt is the resolution in time delay measurements. The resolution in the loss coefficient ($\Delta\alpha$) is given by

$$\Delta\alpha = \frac{2}{l}\left|\ln\left\{1 - \frac{2\Delta A}{A}\right\}\right| + 2\alpha\frac{\Delta l}{l} \quad (15)$$

where $\Delta A/A$ is the relative amplitude stability of the laser system. We estimate Δt to be 0.2 ps in our experiments. The uncertainty in the sample thicknesses is due mainly to the nonuniformity of the samples, and a 0.1 mm difference was measured from the middle to the edges of some of the samples. With a value of $\Delta l = 0.1$ mm we obtain a resolution in the refractive index determination of 2.6% for a 1 cm thickness difference, assuming a nominal index of 2.0. The amplitude stability of the Nd:YAG laser used in our experiments was $\pm 5\%$, giving a resolution in the loss coefficient of 0.2 Np/cm with low-loss samples for which the second term in (15) can be neglected. The Nd:YAG laser was replaced with a more stable Nd:YLF laser, improving the resolution in the loss coefficient to 0.08 Np/cm.

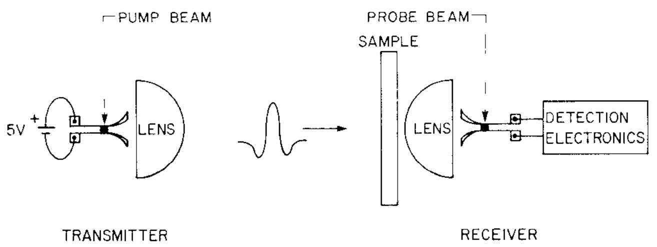

Fig 5. Schematic of the improved experimental setup. Hemispherical lenses are used to collimate and refocus the radiation.

IV. Results and Discussion

The broad-band microwave measurement technique described above has been previously characterized with different structures of well-known and predictable behavior, including a thin metal film on a transparent substrate and Fabry–Pérot interferometers [5]. We now discuss some recent improvements to our experimental setup and present data obtained with the new apparatus.

As mentioned previously the Nd:YAG laser used in our original experiments [5] has been replaced by a Nd:YLF laser. The mode-locked output pulses from the latter are somewhat shorter (~ 30 ps) than those from the former (~ 90 ps) and, after compression and frequency doubling, the optical pulse duration is 1.5 ps. Moreover, the Nd:YLF laser is significantly more stable, with averaged amplitude noise of about $\pm 2\%$, compared with $\pm 5\%$ for the YAG laser. This results in improved sensitivities for measuring loss, as discussed previously. In addition, the antennas used in our original experiments have been replaced with longer structures, having a 10-mm-long feedline and a 5-mm-long radiating section, to increase the delay between the main pulse and the end reflections. This effectively widens the time window over which the experimentally obtained data can be Fourier transformed, thus giving better low-frequency coverage. The end opening of the exponential taper is kept the same as before at 2.6 mm.

As discussed previously, when a noncollimated beam is propagated through a sample a correction is necessary to account for the refraction occurring at the sample surfaces. This correction can be eliminated if a collimated microwave beam is used. This is achieved with 1.0-in-diameter (N.A. = 1.0) hemispheric lenses made of BK-7 glass, as shown in Fig. 5 [19]. Identical lenses are used to collect and collimate the beam diverging from the transmitter, and also to refocus the radiation onto the receiver. The position of the lenses for best collimation is determined experimentally by comparing signal propagation through 0.3175-cm and 1.905-cm-thick pieces of fused silica. Within the accuracy of our measurements this material should show negligible loss, and the best collimation is obtained when the waveforms are identical in all respects except their delay. However, as might be expected for a microwave system involving lenses of this size, the low-frequency (long-wavelength) components of the radiation are not efficiently collected, and in this configuration the low-frequency limit of the measurements is 15 GHz. With

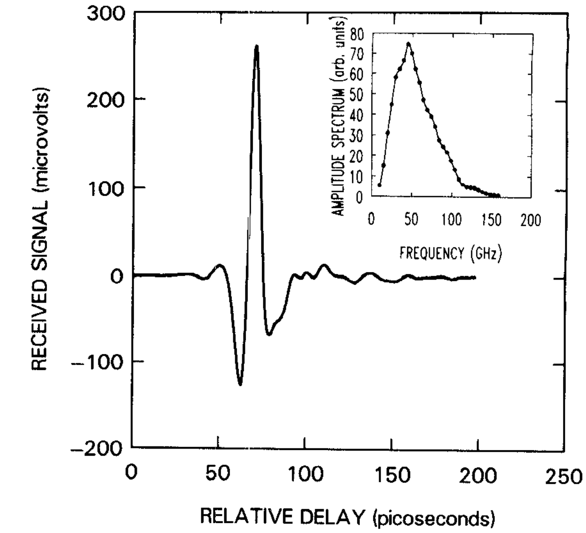

Fig 6. Received waveform obtained with the improved experimental setup, with no sample between the transmitter and the receiver. The corresponding amplitude spectrum is shown in the inset. The dots in the spectrum are determined from experimental data; the continuous line is a guide to the eye.

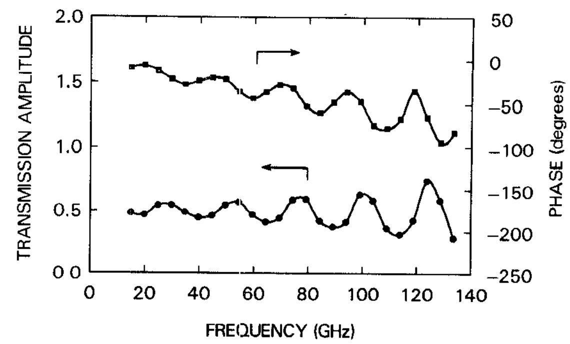

Fig. 7. Amplitude and phase of the transmission function of a Fabry–Pérot interferometer with the two reflecting surfaces 6 mm apart Only the dots correspond to experimental data; the continuous lines are a guide to the eye

collimation, the separation between the transmitter and the receiver can be increased substantially, and measurements are routinely performed with antenna separations of up to 15 cm.

A typical received waveform obtained with the modifications discussed above is shown in Fig. 6 together with its amplitude spectrum. The new experimental apparatus was characterized as before with a thin titanium film on a 10-cm-diameter, 250-μm-thick polished fused silica substrate, and also with Fabry–Pérot interferometers. As expected, both the amplitude $H(f)$ and the phase $\Phi_H(f)$ of the transmission function decreased with frequency for a single Ti-coated substrate. The measured transmission function of a Fabry–Pérot interferometer built with two Ti-coated substrates is shown in Fig. 7, for a plate separation of 6 mm. The modes of a Fabry–Pérot interferometer provide a simple and convenient substitute for a narrow-band absorbing material. The maxima in the amplitude

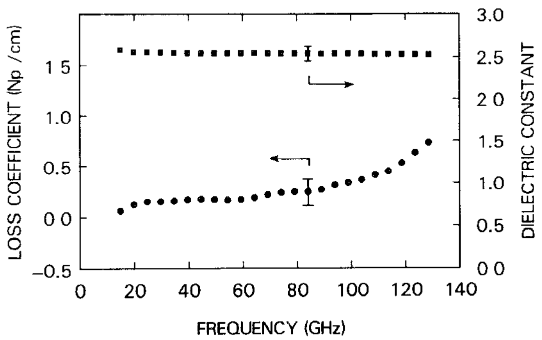

Fig. 8. Loss coefficient and dielectric constant of Plexiglas.

and the corresponding variations in the phase follow the expected behavior for the electric field transmission function [20]. Certain details of the spectra are worth noting. The lower order peaks in the amplitude spectrum appear at frequencies slightly higher than those given by the simple resonance relation $f_N = Nc/2d$, where d is the plate separation. This shift becomes negligible at high frequencies. This is due to the phase shift from the composite reflector, which consists of a thin metal film and a dielectric substrate. It is less than 180° at low frequencies, but approaches 180° at high frequencies. Furthermore, the modulation depth of the modes increases with frequency, since the reflectivity also increases. This is clearly seen in Fig. 7. The validity of the above arguments was confirmed by numerically simulating the Fabry–Pérot measurements with a transmission line analogue of plane wave propagation in stratified media [21]. Excellent agreement was obtained between simulation and data for all the plate separations tested.

The improved setup has been used to characterize the frequency-dependent dielectric properties of several materials, and a representative measurement, for Plexiglas, is shown in Fig. 8. Over the 15–130 GHz spectral range, the loss tangent $\tan\delta$, which is obtained from the loss coefficient by

$$\tan\delta = \frac{\alpha c}{2\pi f n} \tag{16}$$

is less than 0.02 for this material. The physically important quantity, however, is the depicted loss coefficient itself, which can be seen to increase somewhat with frequency. Our measurements are consistent with other data for Plexiglas taken at frequencies higher than 120 GHz [22].

V. Summary

We have described a broad-band microwave measurement technique which is based on the transient radiation from optoelectronically pulsed antennas. Exponentially tapered coplanar stripline antennas are chosen for this application for several of their important characteristics. The radiating elements are integrated with the picosecond optoelectronic devices which are used for photoconductive pulse generation and sampling. The signal analysis that is performed to determine useful material parameters from the received waveforms has also been presented, together with a discussion of the measurement accuracy. We described several improvements to the basic experimental setup and presented results obtained with the modified apparatus.

The COMITS technique has been used to characterize many different substrate materials. The dielectric constants and loss coefficients determined with COMITS can now be used in studying the propagation of electrical pulses on transmission lines fabricated on these substrates. The technique described here provides broad frequency coverage in a region of the electromagnetic spectrum where only relatively narrow-band measurements could formerly be made. Finally, while all the measurements presented here were performed in transmission, COMITS measurements can also be carried out in reflection. This is particularly suitable for lossy materials such as doped semiconductors.

References

[1] C. H. Lee, Ed., *Picosecond Optoelectronic Devices.* Orlando Academic Press, 1984 (and references therein)

[2] P. R Smith, D. H. Auston, and W. M Augustyniak, "Measurement of GaAs field-effect transistor electronic impulse response by picosecond optical electronics," *Appl. Phys. Lett.*, vol 39, pp. 739–741, 1981.

[3] R. K. Jain and D. E. Snyder, "Switching characteristics of logic gates addressed by picosecond light pulses," *IEEE J. Quantum Electron.*, vol. QE-19, pp. 658–663, 1983.

[4] G Arjavalingam, P May, J.-M. Halbout, and G. V. Kopcsay, "Characterization of an experimental thin-film interconnection structure," *SPIE Proc*, vol 947, pp 131–137, 1988

[5] Y. Pastol, G Arjavalingam, J.-M. Halbout, and G V. Kopcsay, "Coherent broadband microwave spectroscopy using picosecond optoelectronic antennas," *Appl. Phys Lett.*, vol. 54, pp. 307–309, 1989

[6] A. H. Harvey, Ed., *Microwave Engineering* London: Academic Press, 1963

[7] F I Shimabukuro and C. Yeh, "Attenuation measurement of very low-loss dielectric waveguides by the cavity resonator method applicable in the millimeter/submillimeter wavelength range," *IEEE Trans. Microwave Theory Tech.*, vol. 36, pp. 1160–1166, 1988

[8] M. N. Afsar, "Dielectric measurements of millimeter-wave materials," *IEEE Trans. Microwave Theory Tech*, vol MTT-32, pp. 1598–1609, 1984.

[9] A. P. DeFonzo, and C R. Lutz, "Optoelectronic transmission and reception of ultrashort electrical pulses," *Appl. Phys Lett.*, vol 51, pp. 212–214, 1987; and P R Smith, D H. Auston, and M. C Nuss, "Subpicosecond photoconducting dipole antennas," *IEEE J Quantum Electron.*, vol 24, pp. 255–260, 1988

[10] Y. Pastol, G Arjavalingam, J-M. Halbout, and G. V. Kopcsay, "Characterization of an optoelectronically pulsed broadband microwave antenna," *Electron Lett*, vol. 24, pp 1318–1319, 1988

[11] M. B Ketchen *et al*, "Generation of subpicosecond electrical pulses on coplanar transmission lines," *Appl Phys Lett.*, vol 48, pp. 751–753, 1986.

[12] F. E Doany, D. R Grischkowsky, and C. C. Chi, "Carrier lifetime versus ion-implantation dose in silicon on sapphire," *Appl Phys. Lett.*, vol. 50, pp. 460–462, 1986

[13] D H. Auston, "Picosecond optoelectronic switching and gating in silicon," *Appl. Phys. Lett.*, vol. 26, pp. 101–103, 1975.

[14] K S Yngvesson *et al.*, "Endfire tapered slot antennas on dielectric substrates," *IEEE Trans. Antennas Propagat.*, vol AP-33, pp. 1392–1400, 1985

[15] P. G. May, J.-M Halbout, and G. L-T Chiu, "Noncontact high-speed waveform measurements with the picosecond photoelectron scanning electron microscope," *IEEE J. Quantum Electron.*, vol. 24, pp. 234–239, 1988

[16] M. Schwartz, *Information Transmission, Modulation and Noise.* Tokyo: McGraw-Hill, 1970.

[17] G. W. Chantry, *Long Wave Optics*, vol. 1. Orlando: Academic Press, 1984, pp. 237–242.

[18] G. J. Davies, "Some aspects affecting the precise measurement of the submillimeter spectra of very low loss dielectrics," *IEEE Trans. Instrum. Meas.*, vol. IM-23, pp. 479–483, 1974.

[19] D. B. Rutledge, D. P. Neikirk, and D. P. Kasilingam, "Integrated circuit antennas," in *Infrared and Millimeter Waves*, K. J. Button, Ed., vol. 10, Pt. II. New York: Academic Press, 1983, pp. 1–90.

[20] E. Hecht and A. Zajac, *Optics.* Reading: Addison-Wesley, 1974, p. 305.

[21] S. Ramo, J. R. Whinnery, and T. Van Duzer, *Fields and Waves in Communication Electronics.* New York: Wiley, 1965, sections 6.10 and 11.06.

[22] J. R. Birch, J. D. Dromey, and J. Lesurf, "The optical constants of some common low-loss polymers between 4 and 40 cm^{-1}," *Infrared Phys.*, vol. 21, pp. 225–228, 1981.

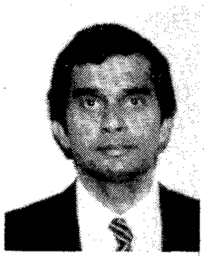

G. Arjavalingam (S'80–M'83) was born in Colombo, Sri Lanka, in March 1957. He obtained the B.A. degree from Cambridge University, U.K., in 1978 and the M.S. and Ph.D. degrees from the University of California, Berkeley, in 1980 and 1983, respectively, all in electrical engineering. His doctoral work was on the production of ultrashort light pulses with mode-locked lasers.

Since 1983 he has been at the IBM Thomas Watson Research Center, Yorktown Heights, NY, where he has worked on the amplification of ultraviolet subpicosecond pulses and various applications of short pulse technology. His most recent work involves the electrical characterization of computer interconnect structures and the materials used to fabricate them. He is currently manager of package measurements at IBM's Thomas J. Watson Research Center.

Dr. Arjavalingam is a member of the Optical Society of America.

Yvon Pastol was born in Lannion, France, on June 27, 1961. He received the Engineer degree from the Institut Supérieur d'Electronique de Paris in 1983 and the Ph.D. in solid-state physics from the University of Paris in 1987.

He then joined the IBM Research Division as a postdoctoral fellow at the Thomas J. Watson Research Center, Yorktown Heights, NY, where he is currently involved in the development of spectroscopy techniques using optoelectronically generated microwave transient radiation.

Jean-Marc Halbout (M'87) received the "Ingenieur" degree from the Institut Supérieur d'Electronique de Paris in 1977 and the Ph.D. degree in electrical engineering from Cornell University, Ithaca, NY, in 1981.

Since 1983 he has been with the IBM Research Division at the Thomas J. Watson Research Center, Yorktown Heights, NY. His research interests include the applications of ultrashort optical and electrical pulses to the study of ultrafast phenomena in optical and electronic devices. Since 1988 he has been Manager of the Ultrafast Measurements Group in the Advanced Silicon Technology Department.

Dr. Halbout is a member of the Optical Society of America and the Lasers and Electro-Optics Society.

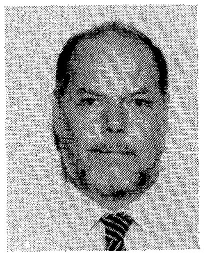

Gerard V. Kopcsay (S'68–M'69) holds the B.E. and M.S. degrees in electrical engineering.

He is a Research Member in the Packaging Technology Department at the IBM Thomas J. Watson Research Center, Yorktown Heights, NY. Since joining IBM Research in 1978, he has been working on the analysis and design of high-performance computer packaging. From 1969 to 1978 he worked on research and development of low-noise microwave receivers at the AIL Division of Eaton Corp.

Mr. Kopcsay is a member of the IEEE and the American Physical Society.